# Supplementary materials

Zhenfei Ma[1], Xiankui Yang[5], Jiangtao Zhu[5], Xingjian Kong[*2,3] ,Pan Zhang[*4]

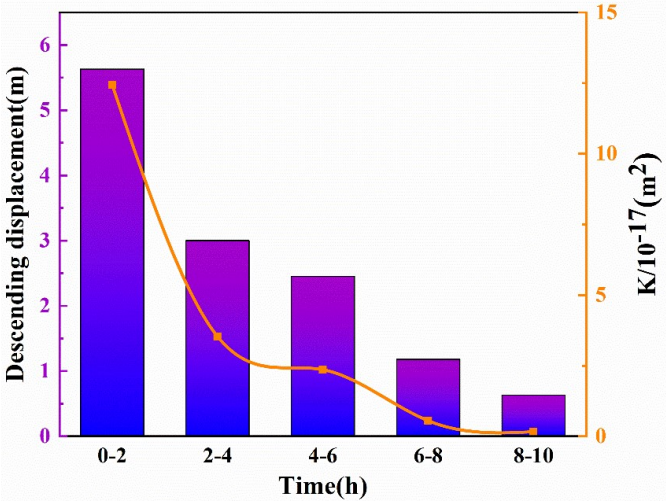


Fig.S1 The change of permeability coefficient of asphalt with time

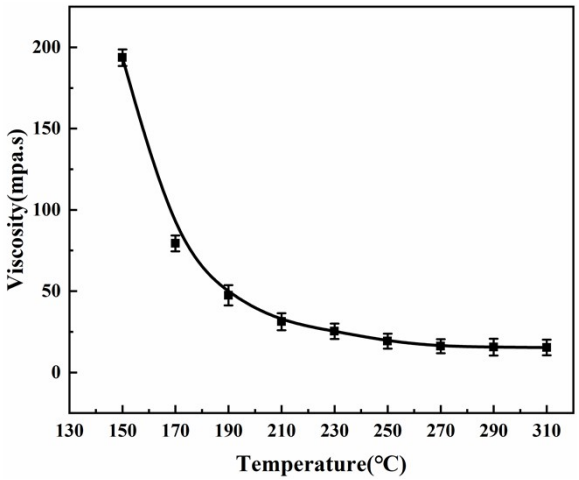


Fig.S2 Viscosity-temperature curve of asphalt

1. Purification Equipment Research Institute of CSSC, Handan, China
2. Chemical Science and Engineering College, Sichuan University, Chengdu 610065, China, P R 3. Engineering Research Center of Comprehensive Utilization and Clean Processing of Phosphorus, Chengdu 610065, China, P R
4.College of Chemical Engineering, Sichuan University of Science & Engineering, Zigong 643000, China.
5. Peric Special Gases Co., Ltd., Handan 056002 Hebei， China
*Corresponding author: Xingjian Kong; Pan Zhang; E-mail address: kongxingjian@scu.edu.cn; 18381314085@163.com

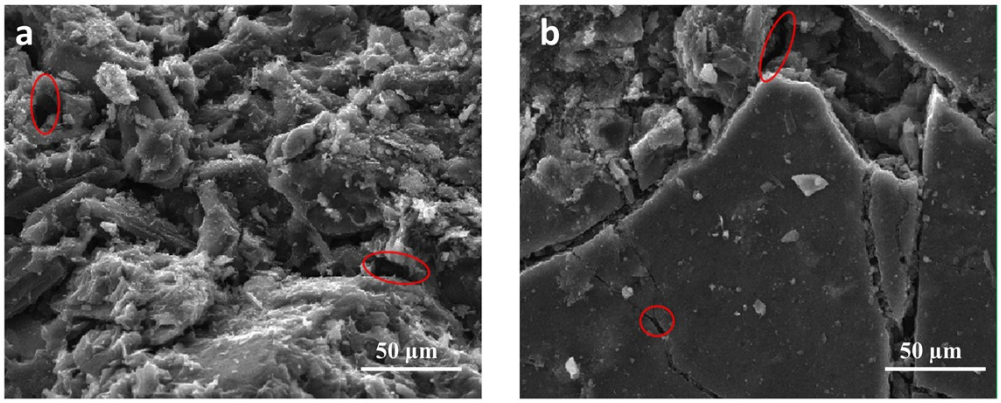


Fig. S3 Fracture and surface morphology of carbon anode

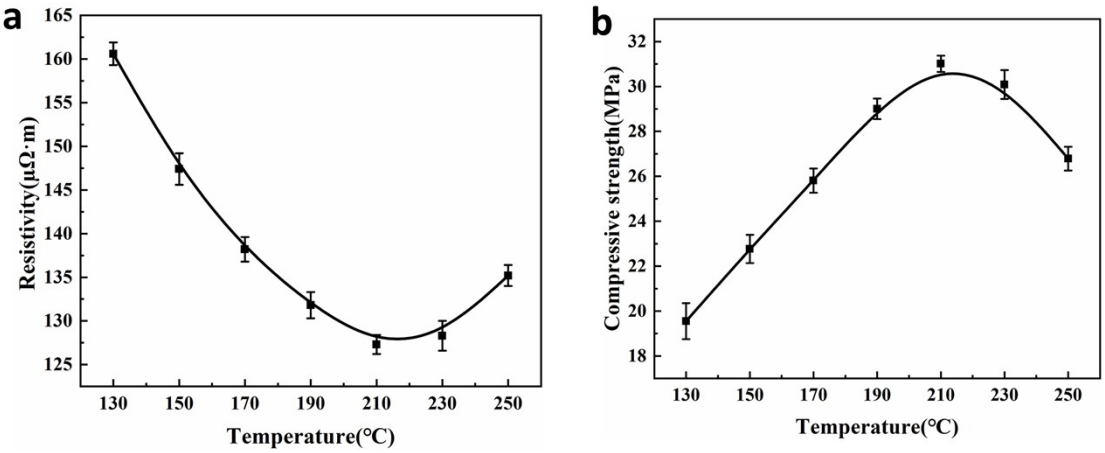


Fig. S4 (a) Influence of impregnation temperature on resistivity of preform;(b) Influence of impregnation temperature on compressive strength of preform

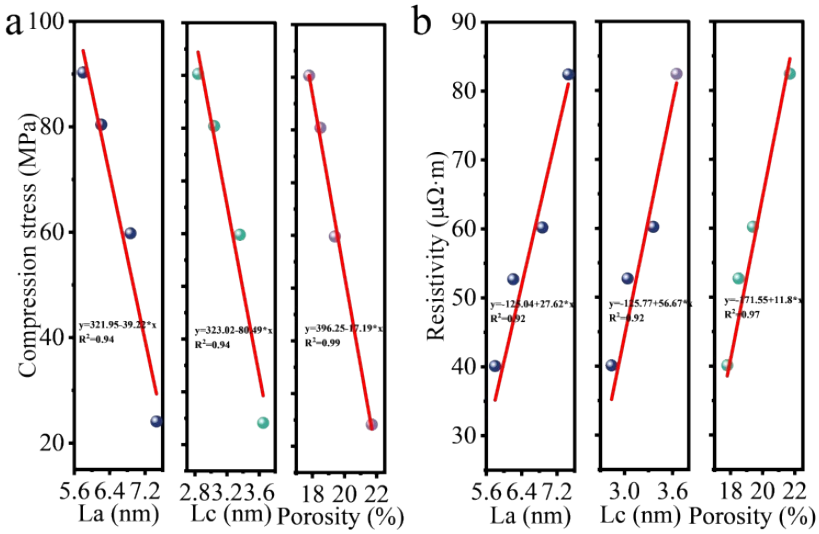


Fig.S5. Relation curves of the compression stress:(a)La、Lc and Porosity; Relation curves of the resisitivity:(b)La、Lc and Porosity.

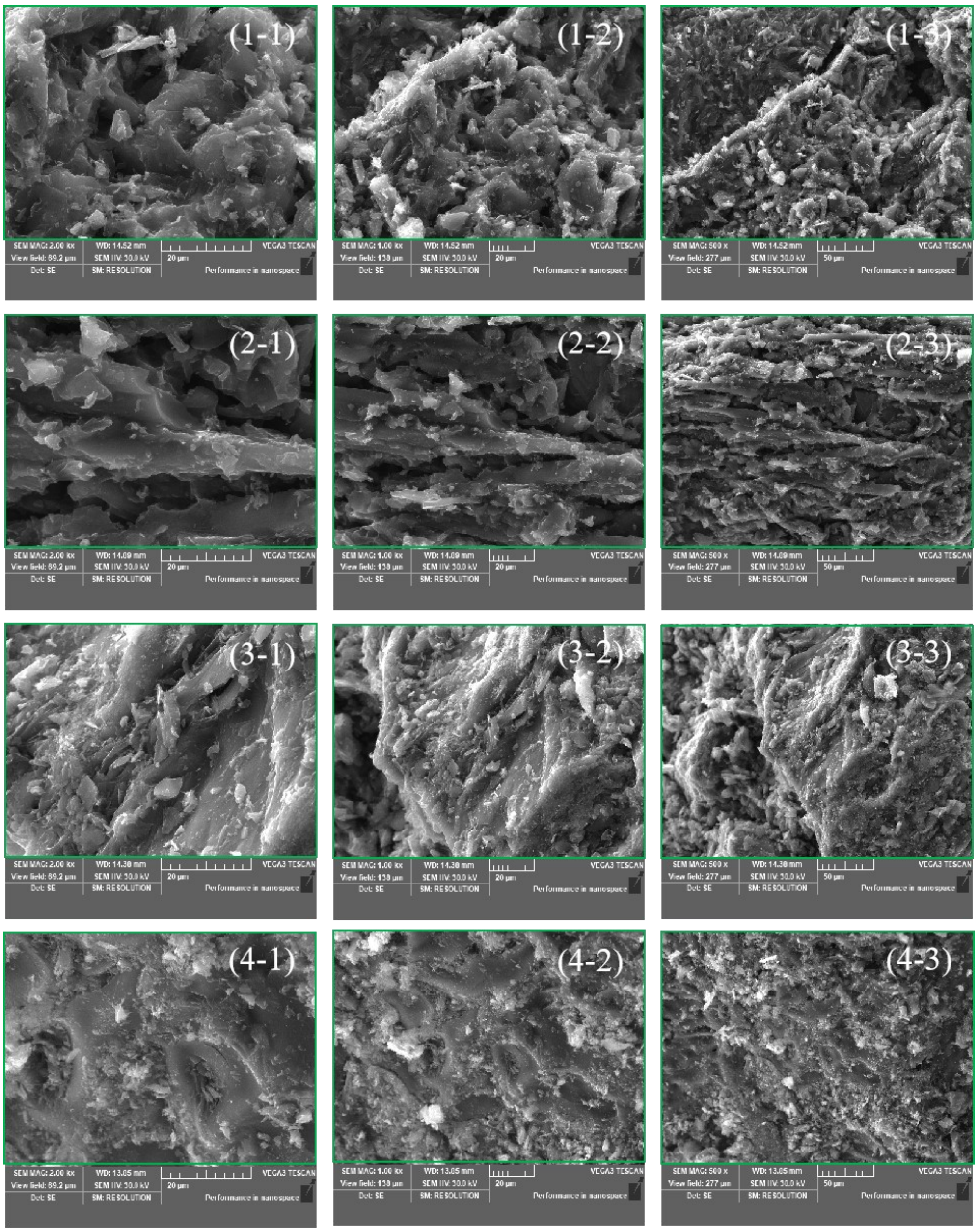


Fig. S6 Fracture morphology of prefabricated body

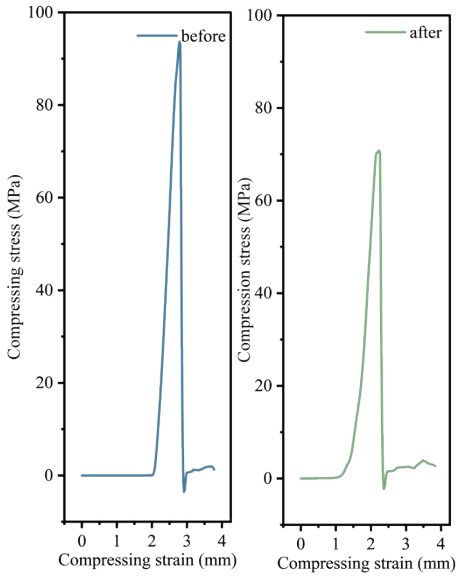


Fig.S7 Mechanical properties of the carbon anodes before and after Electrolysis

Table-S1 Carbonization time at different temperatures

| number | carbonization time (min) | | | |
|---|---|---|---|---|
| | 0~300 ℃ | 300~400 ℃ | 400~500 ℃ | 500 ℃ |
| A1 | 30 | 240 | 100 | 30 |
| A2 | 30 | 240 | 120 | 30 |
| A3 | 30 | 240 | 140 | 30 |
| A4 | 30 | 240 | 160 | 30 |
| A5 | 30 | 240 | 180 | 30 |
| A6 | 30 | 240 | 200 | 30 |
| B1 | 30 | 200 | 180 | 30 |

| | | | | |
|---|---|---|---|---|
| B2 | 30 | 220 | 180 | 30 |
| B3 | 30 | 240 | 180 | 30 |
| B4 | 30 | 260 | 180 | 30 |
| B5 | 30 | 280 | 180 | 30 |
| B6 | 30 | 300 | 180 | 30 |
| C1 | 30 | 240 | 180 | 30 |
| C2 | 50 | 240 | 180 | 30 |
| C3 | 70 | 240 | 180 | 30 |
| C4 | 90 | 240 | 180 | 30 |
| C5 | 110 | 240 | 180 | 30 |
| C6 | 130 | 240 | 180 | 30 |
| D1 | 30 | 240 | 180 | 30 |
| D2 | 30 | 240 | 180 | 50 |
| D3 | 30 | 240 | 180 | 70 |
| D4 | 30 | 240 | 180 | 90 |
| D5 | 30 | 240 | 180 | 110 |
| D6 | 30 | 240 | 180 | 130 |

Table-S2 Comparison of parameters of different carbon anode preparation processes

| | impregnation time (h) | carbonization time (h) | maximum carbonization temperature (℃) | Cycle (times) |
|---|---|---|---|---|
| new route | 2 | 48 | 500 | 4 |
| traditional route | 1 | 54 | 1200 | 2 |

Table-S3 Lattice parameters of preforms under different cycles of impregnation and carbonization

| impregnation–carbonization stage | $2\theta_{002}$ | $d_{002}$(nm) | La(nm) | Lc(nm) |
|---|---|---|---|---|

| | | | | |
|---|---|---|---|---|
| 1-1st | 25.84 | 0.3447 | 7.46 | 3.65 |
| 2-2nd | 25.74 | 0.3460 | 6.87 | 3.36 |
| 3-3rd | 25.69 | 0.3467 | 6.21 | 3.04 |
| 4-4th | 25.61 | 0.3477 | 5.80 | 2.84 |

Table-S4 Prefabricated body blank for test

| Cycle | densification process | preform volume ($cm^3$) | preform density ($g/cm^3$) |
|---|---|---|---|
| 1-1$^{st}$cycle | liquid-phase impregnation | 3.847 | 1.630 |
| 2-2$^{nd}$cycle | liquid-phase impregnation | 4.460 | 1.707 |
| 3-3$^{rd}$cycle | liquid-phase impregnation | 4.402 | 1.748 |
| 4-4$^{th}$cycle | liquid-phase impregnation | 5.043 | 1.773 |

Table-S5 Prefabricated test block (1-1$^{st}$cycle) density distribution

| number | test block size (mm) | | volume | mass | density |
|---|---|---|---|---|---|
| | diameter | height | ($cm^3$) | (g) | ($g/cm^3$) |
| **0#** | 20.17 | 12.04 | 3.847 | 6.271 | 1.630 |
| **1#** | 20.17 | 10.64 | 3.400 | 5.528 | 1.626 |
| **2#** | 20.17 | 9.24 | 2.952 | 4.776 | 1.618 |
| **3#** | 20.17 | 7.82 | 2.499 | 4.071 | 1.629 |
| **4#** | 20.17 | 6.42 | 2.051 | 3.337 | 1.627 |

Table-S6 Prefabricated test block (2-2$^{nd}$cycle) density distribution

| number | test block size (mm) | | volume | mass | density |
|---|---|---|---|---|---|
| | diamete | height | ($cm^3$) | (g) | ($g/cm^3$) |
| **0#** | 20.19 | 14.02 | 4.460 | 7.613 | 1.707 |
| **1#** | 20.19 | 12.61 | 4.037 | 6.802 | 1.685 |
| **2#** | 20.19 | 11.21 | 3.589 | 6.076 | 1.693 |

| | | | | | |
|---|---|---|---|---|---|
| **3#** | 20.19 | 9.83 | 3.147 | 5.331 | 1.694 |
| **4#** | 20.19 | 8.43 | 2.699 | 4.556 | 1.688 |
| **5#** | 20.19 | 7.03 | 2.251 | 3.788 | 1.683 |

Table-S7 Prefabricated test block (3-3rdcycle) density distribution

| number | test block size (mm) | | volume | mass | density |
|---|---|---|---|---|---|
| | diamete | height | ($cm^3$) | (g) | ($g/cm^3$) |
| **0#** | 20.16 | 13.79 | 4.402 | 7.695 | 1.748 |
| **1#** | 20.16 | 12.39 | 3.955 | 6.874 | 1.738 |
| **2#** | 20.16 | 10.99 | 3.508 | 6.086 | 1.735 |
| **3#** | 20.16 | 9.61 | 3.068 | 5.277 | 1.720 |
| **4#** | 20.16 | 8.21 | 2.621 | 4.526 | 1.727 |
| **5#** | 20.16 | 6.81 | 2.174 | 3.750 | 1.725 |

Table S8 Prefabricated test block (4-4rdcycle) density distribution

| number | test block size (mm) | | volume | mass | density |
|---|---|---|---|---|---|
| | diameter | height | ($cm^3$) | (g) | ($g/cm^3$) |
| **0#** | 20.09 | 15.91 | 5.043 | 8.941 | 1.773 |
| **1#** | 20.09 | 14.51 | 4.600 | 8.105 | 1.762 |
| **2#** | 20.09 | 13.11 | 4.156 | 7.306 | 1.758 |
| **3#** | 20.09 | 11.70 | 3.709 | 6.513 | 1.756 |
| **4#** | 20.09 | 10.30 | 3.265 | 5.720 | 1.752 |
| **5#** | 20.09 | 8.91 | 2.824 | 4.922 | 1.743 |
| **6#** | 20.09 | 7.51 | 2.381 | 4.121 | 1.731 |

Table-S9 Carbon anode quality index comparison

| type | bulk density ($g/cm^3$) | resistivity ($\mu\Omega\cdot m$) | compressive strength (MPa) | Ash (%) | porosity (%) |
|---|---|---|---|---|---|
| new route | 1.793 | 32.1 | 89.7 | 0.5 | 17.8 |
| traditional | 1.814 | 29.8 | 89.3 | 0.5 | 17.5 |

| route | | | | | |
|---|---|---|---|---|---|
| Russia | 1.640 | 25.0~40.0 | 58.8 | 0.6 | 21.0 |
| Germany | 1.600 | 46.0 | 95.9 | 0.4 | 15.3 |
| France | 1.680 | 45.0 | 95.9 | 0.4 | 15.3 |
| Japan | 1.810 | 25.0 | 59.0 | 0.1 | 23.0 |
| China | 1.700 | 45.0 | 70.0 | 0.3 | 27.0 |